Influence of the direction of spontaneous orientation polarization on the charge injection properties of organic light-emitting diodes

Yutaka Noguchi' , Hyunsoo Lim, Takashi Isoshima, Eisuke Ito, Masahiko Hara, Whee Won Chin, Jin Wook Han, Hiroumi Kinjo, Yusuke Ozawa, Yasuo Nakayama, and Hisao Ishii'

Citation: Appl. Phys. Lett. **102**, 203306 (2013); doi: 10.1063/1.4807797
View online: http://dx.doi.org/10.1063/1.4807797
View Table of Contents: http://aip.scitation.org/toc/apl/102/20
Published by the American Institute of Physics

Influence of the direction of spontaneous orientation polarization on the charge injection properties of organic light-emitting diodes

Yutaka Noguchi,[1,2,a)] Hyunsoo Lim,[2] Takashi Isoshima,[3] Eisuke Ito,[3] Masahiko Hara,[3] Whee Won Chin,[4] Jin Wook Han,[4] Hiroumi Kinjo,[2] Yusuke Ozawa,[2] Yasuo Nakayama,[1] and Hisao Ishii[1,2,b)]

[1]*Center for Frontier Science, Chiba University, 1-33 Yayoi-cho, Inage, Chiba 263-8522, Japan*
[2]*Graduate School of Advanced Integration Science, Chiba University, 1-33 Yayoi-cho, Inage-ku, Chiba 263-8522, Japan*
[3]*Flucto-Order Functions Research Team, RIKEN-HYU Collaboration Research Center, RIKEN Advanced Science Institute, Wako, Saitama 351-0198, Japan*
[4]*Department of Chemistry, Hanyang University, Seoul 133-791, South Korea*

(Received 24 March 2013; accepted 13 May 2013; published online 24 May 2013)

A tris(7-propyl-8-hydroxyquinolinato) aluminum [Al(7-Prq)$_3$] film shows negative giant surface potential (GSP) because of spontaneous orientation polarization. The polarity of this film is opposite to those of tris-(8-hydroxyquinolate) aluminum films. In Al(7-Prq)$_3$-based organic light-emitting diodes, negative GSP leads to the *positive* interface charge and governs the *electron* injection and accumulation properties. In addition, a high resistance to the *electron* injection at the Al(7-Prq)$_3$/Ca interface is suggested possibly because of the negative polarization charge at the interface. These results show the importance of orientation polarization in controlling the charge injection and accumulation properties and potential profile of the resultant devices. © *2013 AIP Publishing LLC*. [http://dx.doi.org/10.1063/1.4807797]

Some organic semiconducting materials are spontaneously ordered in evaporated films even though the films are typically regarded as amorphous.[1,2] Molecular order significantly affects the optical and electrical properties of the resultant devices. In particular, if molecules possess a permanent dipole moment, the ordered films can lead to a spontaneous orientation polarization. The surface potential of such polar films grows linearly as a function of the film thickness, and it typically reaches several to ten volts for a 100-nm-thick film.[2] This anomalous increase in surface potential (giant surface potential, GSP) was first observed in evaporated films of tris-(8-hydroxyquinolate) aluminum (Alq_3) by Ito *et al.*,[3] and subsequent studies revealed similar behavior in several materials commonly used in organic light-emitting diodes (OLEDs), such as metal complexes,[4] bathocuproine (BCP),[5] 1,3,5-tris(1-phenyl-1H-benzimidazol-2-yl)benzene (TPBi),[6] 1,3-bis[2-(4-tert-butylphenyl)-1,3,4-oxadiazo-5-yl] benzene (OXD-7), and 4, 4′-bis[*N*-(1-naphthyl)-*N*-phenylamino]-biphenyl (α-NPD).[2] The polarity of GSP in the previous studies has been mostly *positive* with respect to the substrate potential, indicating that the direction of the permanent dipole moment of the molecules points to the surface normal on average (a positive polarization charge appears on the film surface), and the mechanism of the formation of the spontaneous orientation polarization in the film remains to be clarified.[2,7,8] However, Isoshima *et al.* recently reported that the attachment of a propyl group to Alq_3 leads to an inverted polarity of GSP.[9] This result strongly suggests that the molecular shape is critical to form the orientation polarization in the evaporated film.

Because of the photoinduced decay nature,[3,5,10,11] GSP has not been considered as an important parameter in terms of device properties; however, the orientation polarization is maintained in the actual devices and induces a negative polarization charge at the heterojunctions in these devices.[2,12] The negative interface charge governs the hole injection and accumulation properties.[13] The hole injection occurs at biases even lower than the built-in voltage (V_{bi}) of a device because of the electric field formed by the interface charge. The injected charges are captured at the heterojunction until the interface charge is compensated; i.e., the interface charge density determines the minimum accumulated charge during the device operation. The interface charge density is typically as high as ~ -1 mC/m^2, which is a significant amount for the total accumulated charge density of the device under operation.[14–18] Because the charge accumulation in multilayer OLEDs affects the device operation, efficiency, and degradation properties,[14,19–22] the elucidation of the influence of polar films on the device properties and development of methods to control orientation polarization are important in achieving improved device performance.

In this study, we report that a derivative of Alq_3, tris(7-propyl-8-hydroxyquinolinato) aluminum [Al(7-Prq)$_3$], shows a negative GSP with a slope of -103 mV/nm for a film evaporated onto an indium-tin oxide (ITO) substrate; the potential of this film is a few times greater than those of GSP films reported previously with the opposite polarity, e.g., 33 mV/nm for an Alq_3 film. In Al(7-Prq)$_3$-based bilayer OLEDs, negative GSP leads to a *positive* interface charge and governs the *electron* injection and accumulation properties. The interface charge density and polarity estimated from the displacement current measurement (DCM) curves show trends similar to that of the polarization charge density obtained from the Kelvin probe (KP) measurements. In

[a)]Electronic address: y-noguchi@faculty.chiba-u.jp
[b)]Electronic address: ishii130@faculty.chiba-u.jp

addition, the DCM curve suggests a high contact resistance for the *electron* injection at the Al(7-Prq)$_3$/Ca interface possibly because of the presence of the negative polarization charge at the interface. These results suggest that the spontaneous orientation polarization is an important factor with respect to device performance. Furthermore, combinations of positive and negative GSP films will allow us to actively design the potential profile in multilayer organic semiconductor devices without doping. We therefore expect that the GSP films could open another path for achieving desirable potential profiles in organic devices.

Figure 1(a) shows molecular structures of Al(7-Prq)$_3$ and Alq$_3$. A propyl group is attached to the 7-position of the quinolinolate ligand for Al(7-Prq)$_3$. The permanent dipole moment (p) of these molecules in the meridional form is estimated to be 3.75 D for Al(7-Prq)$_3$ and 4.41 D for Alq$_3$ on the basis of quantum chemical calculations (Gaussian 03 with a basis set of B3LYP/6-31 G(d)). The peak in the optical absorption and photoluminescence (PL) spectra (λ_{abs} and λ_{PL}, respectively) of Al(7-Prq)$_3$ are slightly red-shifted with respect to those of Alq$_3$ [Figs. 1(b) and 1(c)], as previously reported.[9,23] The fluorescence quantum yield (η_f) of Al(7-Prq)$_3$ in powder form, used as the evaporation source, is approximately half that of Alq$_3$. The ionization energies of the evaporated films (I) is estimated to be 5.8 ± 0.1 eV and 5.7 ± 0.1 eV for Al(7-Prq)$_3$ and Alq$_3$, respectively, by photoelectron yield spectroscopy (PYS). On the basis of the ionization energy and optical absorption spectra, an energy diagram of these molecules with the highest occupied molecular orbital (HOMO) level of α-NPD[24] and a work function of Ca is presented in Fig. 1(d), where a common vacuum level at the contacts is assumed.[25] The basic properties of these molecules are summarized in Table I.

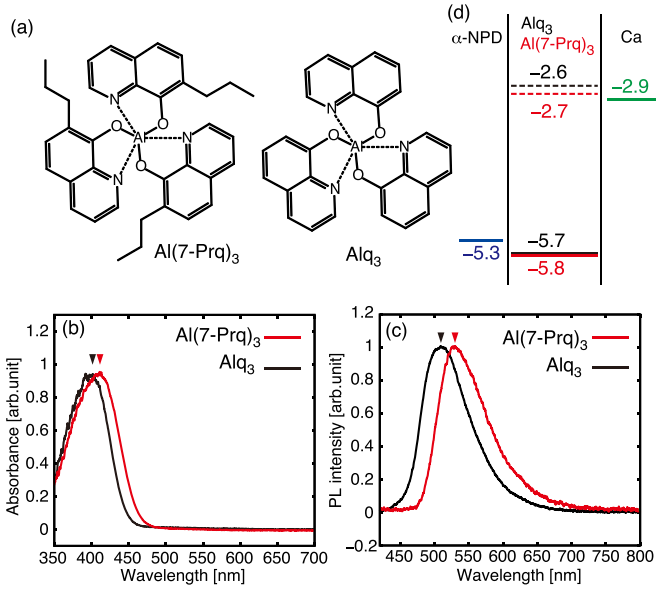

FIG. 1. (a) Chemical structures of Al(7-Prq)$_3$ (left) and Alq$_3$ (right). (b) Optical absorption spectra of Al(7-Prq)$_3$ and Alq$_3$ in acetone solution. (c) Photoluminescence spectra of Al(7-Prq)$_3$ and Alq$_3$ in powder form. (d) Schematic energy diagram of the α-NPD/Al(7-Prq)$_3$ and Alq$_3$/Ca structures (unit: eV). HOMO levels (solid lines) are determined from the PYS measurements. LUMO levels (broken lines) are assumed from the optical energy gap and HOMO level.

TABLE I. Basic properties of Al(7-Prq)$_3$ and Alq$_3$.

Compound	p [D]	I [eV]	λ_{PL} [nm]	λ_{abs} [nm]	GSP [mV/nm]	ε_r	σ_{int} [mC/m^2]
Al(7-Prq)$_3$	3.75	5.8 ± 0.1	529	410	−103	2.0	3.1
Alq$_3$	4.41	5.7 ± 0.1	509	398	33	3.2	−1.1

Figure 2 shows the current-density–voltage–luminance (J–V–L) characteristics of the ITO/α-NPD (70 nm)/Al(7-Prq)$_3$ or Alq$_3$ (50 nm)/Ca/Al devices. The luminous efficiency of the Al(7-Prq)$_3$ device is approximately 60% that of the Alq$_3$ device. This diminished luminous efficiency can be mostly attributed to the low η_f of Al(7-Prq)$_3$; the contributions of other factors such as the charge balance, light outcoupling, and radiative recombination coefficient may not be significant. The conductance of the Al(7-Prq)$_3$ device, however, is remarkably low, which indicates low charge carrier mobilities of the Al(7-Prq)$_3$ film and a high resistance to the charge injection at the interfaces, e.g., α-NPD/Al(7-Prq)$_3$ for holes and Al(7-Prq)$_3$/Ca for electrons. The charge carrier mobilities of the Al(7-Prq)$_3$ film are not examined, although an overlap of molecular orbitals, e.g., the HOMO and lowest unoccupied molecular orbital (LUMO), between neighboring molecules may be hindered by the propyl group. A high resistance to the electron injection at the Al(7-Prq)$_3$/Ca interface is suggested by the DCM curves, as discussed later.

Figure 3 shows the surface potentials of the Al(7-Prq)$_3$ and Alq$_3$ films formed on the ITO substrate as a function of the film thickness. The surface potential is measured *in situ* at each step of the film deposition under high-vacuum conditions using the KP method with reference to the work function of the ITO substrate. Here, measurements are performed in the absence of light to avoid alteration of surface potential by photocarriers generated in the film.[3] The surface potential of the Al(7-Prq)$_3$ film clearly exhibits GSP behavior with a slope of −103 mV/nm (Fig. 3). This value is approximately three times greater than that of the Alq$_3$ film on ITO (33 mV/nm) and is

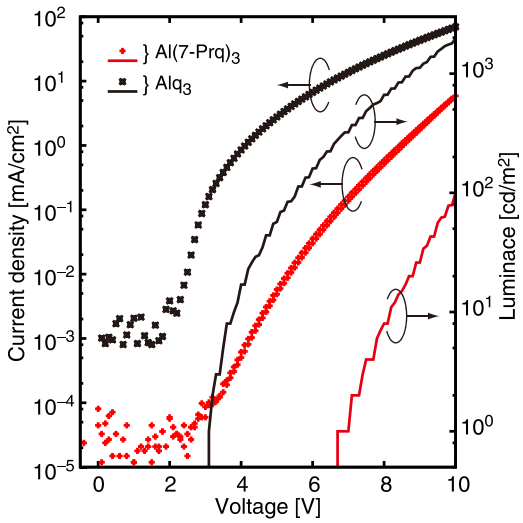

FIG. 2. Current density–voltage–luminance (J–V–L) characteristics of ITO/α-NPD/Al(7-Prq)$_3$ or Alq$_3$/Ca/Al devices. The maximum luminous efficiency of the Al(7-Prq)$_3$ device was 1.7 cd/A, whereas that of the Alq$_3$ device was 2.8 cd/A.

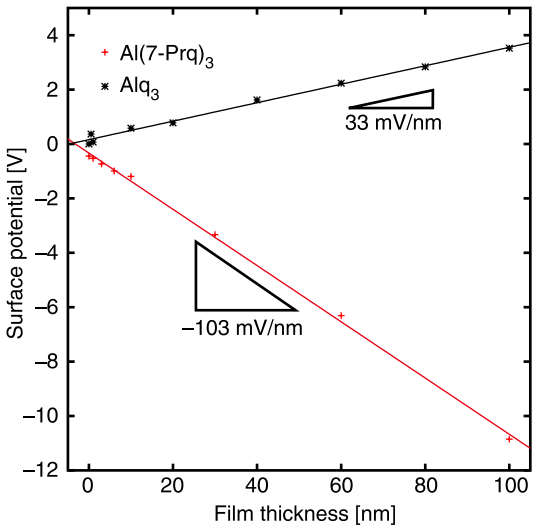

FIG. 3. Surface potential of $Al(7\text{-}Prq)_3$ and Alq_3 films evaporated onto an ITO substrate.

similar to the previously reported value (−118 mV/nm).[9] Remarkably, GSP of the $Al(7\text{-}Prq)_3$ film increases negatively, indicating that the direction of the permanent dipole moment of $Al(7\text{-}Prq)_3$, on average, points to the substrate in the evaporated film, whereas that of Alq_3 points to the film surface. A polarization charge with a constant density of 1.82 mC/m^2 is induced behind the $Al(7\text{-}Prq)_3$ film (substrate side) using a dielectric constant (ε_r) of 2. Here, the charge density (σ) was estimated by Poisson's equation: $\sigma = \varepsilon_0\varepsilon_r V_s/d$, where ε_0 is the dielectric permittivity of vacuum, V_s is the surface potential, and d is the film thickness. ε_r was estimated from the capacitance measurement of the $Al(7\text{-}Prq)_3$ devices. The small dielectric constant of $Al(7\text{-}Prq)_3$ film may originate from the low film density.[9]

We perform DCM on the ITO/α-NPD/$Al(7\text{-}Prq)_3$/Ca/Al device to examine the influence of the opposite orientation polarization of the $Al(7\text{-}Prq)_3$ film on the charge injection and accumulation properties of $Al(7\text{-}Prq)_3$-based devices. DCM is a type of capacitance–voltage (C–V) measurement that uses a triangular waveform as the applied voltage and measures both the actual and displacement current responses.[7] Because of the constant sweep rate of the applied voltage (dV/dt), i_{dis} is proportional to the apparent capacitance of the test device (C_{app}). The accumulation charge density can be estimated by integrating the measured C_{app} along the V axis if the sweep rate is sufficiently slow (i.e., the quasi-static regime).

Figure 4(a) shows the DCM curve of an $Al(7\text{-}Prq)_3$-based device, where the sweep rate is 1 V/s. Depletion, intermediate, and accumulation states clearly appear in the DCM curve [(i), (ii), and (iii) in Fig. 4(a), respectively].[7] In the forward sweep, the onset of the charge injection appears at approximately −8 V [V_{inj} in Fig. 4(a)], and the injected charge accumulates at the α-NPD/$Al(7\text{-}Prq)_3$ interface. In contrast, the discharging process of the accumulated charge is observed in the backward sweep. Figure 4(b) shows the inverse of C_{app} at the depletion and accumulation states of the bilayer devices with varying $Al(7\text{-}Prq)_3$ film thickness. Although $1/C_{app}$ at the depletion state linearly increases with the $Al(7\text{-}Prq)_3$ film thickness, that at the accumulation

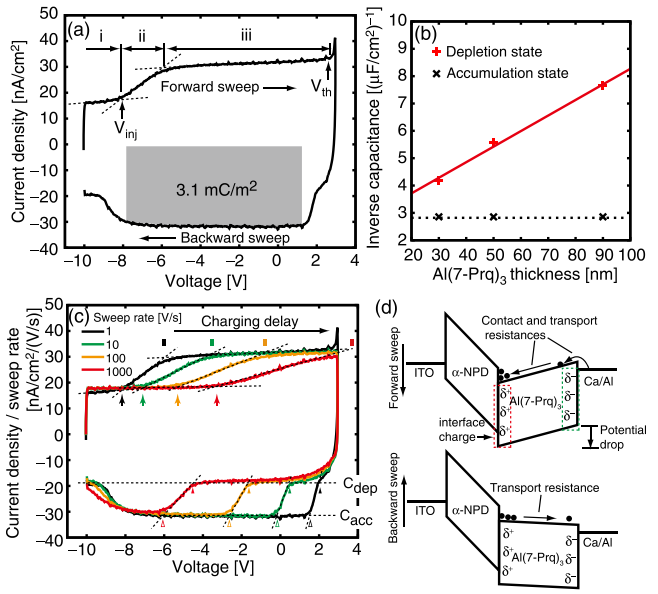

FIG. 4. (a) DCM curves of ITO/α-NPD/$Al(7\text{-}Prq)_3$/Ca/Al device (1 V/s). (i) Depletion, (ii) intermediate, and (iii) accumulation states are observed in the forward sweep. The onset of the charge injection is at approximately −8 V because of the presence of the interface charge. The interface charge density is estimated to be 3.1 mC/m^2 by integrating the displacement current during the charge extraction process (the gray area). (b) Inverse of the apparent capacitance at the depletion and accumulation states as a function of the $Al(7\text{-}Prq)_3$ film thickness. The inverse capacitance at the accumulation state is independent of the film thickness, whereas that at the depletion state is proportional. (c) DCM curves measured at various sweep rates from 1 to 1000 V/s; V_{inj} (arrows) shifts to the higher side, and the intermediate state appears wider at higher sweep rates. In the backward sweep, the discharge process starts at a lower voltage (indicated by the filled triangle) with increasing sweep rate, but immediately reaches C_{acc} (open triangle). (d) Schematic illustrations of the energy diagram of the device at a bias during the forward (top) and backward (bottom) sweeps.

state is constant. We therefore conclude that the α-NPD layer functions as a capacitor at the accumulation state and the injected charge in this bias region is an *electron*. We note that these processes occur at biases lower than the onset of the actual current [2.4 V, V_{th} in Fig. 4(a)], which indicates the presence of *positive* interface charge in the $Al(7\text{-}Prq)_3$-based device.[7,13]

We estimate the positive interface charge density to be approximately 3.1 mC/m^2 by integrating the current during the discharging process [Fig. 4(a)]. Note that the DCM curve is asymmetric to the forward and backward bias sweeps, which suggests that the DCM curve includes the transient current response.[26,27] In other words, the device was not in the quasi-static state even at a sweep rate of 1 V/s. In this case, the estimation of the interface charge density by integrating the DCM curve includes an error of the transient current. We therefore also measured C–V curves of an $Al(7\text{-}Prq)_3$-based device at a very low frequency (1 mHz) and a similar value of 2.7 mC/m^2 was obtained. The following discussions are based on the estimated value from the DCM curve.

The interface charge density of 3.1 mC/m^2 is 2.8 times greater than that of an Alq_3-based bilayer device with opposite polarity.[2,13] Here, the polarization charge density estimated from the GSP slope (1.82 mC/m^2) is smaller than the interface charge density (3.1 mC/m^2). The polarization charge density is likely to be underestimated as GSP decays

irreversibly because of an unexpected counter charge, e.g., charge injected from the electrode, photoinduced carriers, etc.[3,10] Although the quantitative disagreement remains, the results clearly show that negative GSP in the Al(7-Prq)$_3$ film leads to a positive interface charge and determines the polarity of the primary injected carrier and accumulation charge at the hetero interface in the bilayer OLED.

Figure 4(c) shows the DCM curves at various sweep rates from 1 to 1000 V/s. The vertical axis shows the ratio of current density to sweep rate, which corresponds to C_{app}. The curves in the forward sweep significantly distort with an increase in the sweep rate of the applied voltage; the increase in C_{app} is suppressed at higher sweep rates. This result indicates that the electron charging to the hetero interface is delayed because of a long RC time constant (τ_{RC}) of the test device.[7,26,27] Because the carrier of the device in this bias range is an electron, τ_{RC} can be attributed to the high resistance to the electron injection and transport in the Al(7-Prq)$_3$ layer, as suggested by the *J–V* characteristics (Fig. 2). The high resistance results in a potential drop in the Al(7-Prq)$_3$ layer in the forward sweep [Fig. 4(d) top]. In the backward sweep, C_{app} is maintained at approximately C_{dep} at biases greater than a certain voltage [indicated by the filled triangles in Fig. 4(c)], which suggests that the discharge process does not start immediately after the direction of the bias sweep is changed. The discharging process starts after the potential drop decreases with the applied voltage [Fig. 4(d), bottom]. Interestingly, during the discharging process, C_{app} rapidly increases with that of the α-NPD layer (C_{acc}), except when the sweep rate is 1000 V/s [indicated by open triangles in Fig. 4(c)]. These results suggest that τ_{RC} of the discharging process is lower than that of the injection process. The asymmetric τ_{RC} in the forward and backward sweeps can be attributed to the contact resistance, e.g., when the injection barrier for the electron is significant at the Al(7-Prq)$_3$/Ca interface.

If we simply assume that the energy barrier for the electron injection is the difference between the LUMO level and work function of Ca, no significant difference is observed between the Al(7-Prq)$_3$/Ca and Alq$_3$/Ca interfaces [Fig. 1(b)]. Although these are not the accurate barrier height for electron injection in the actual devices, the high contact resistance can be attributed to another origin that is the negative polarization charge at the Al(7-Prq)$_3$/Ca interface. The negative polarization charge induced by the spontaneous orientation polarization [Fig. 4(d)], which is the counter charge of the positive interface charge at the α-NPD/Al(7-Prq)$_3$ interface. The presence of the negative charge can suppress the electron injection from the cathode to the Al(7-Prq)$_3$ layer. Similarly, at the α-NPD/Al(7-Prq)$_3$ interface, the hole injection to the Al(7-Prq)$_3$ layer can be suppressed. We recently reported a similar phenomenon at the organic heterojunctions in the bilayer systems of polar or non-polar films on an α-NPD layer.[24] An ultraviolet photoelectron spectroscopy study revealed that the electron transfer is unlikely to occur at the heterojunctions if the polar films such as TPBi and OXD-7 are used as overlayers (in the case of TPBi and OXD-7, the *negative* interface charge exists at the heterojunction). These results suggest that the charge transfer can be suppressed by the polarization charge. The polarity of orientation polarization can play an important role in the efficient charge injection, and a film with a positive orientation polarization, which corresponds to a positive polarization charge at the film surface, could be used as an electron injection layer (EIL). The use of Alq$_3$, BCP, TPBi, and OXD-7 layers as EILs is therefore a reasonable choice in terms of the polarity of the film.

In summary, we examined the influence of negative GSP in an evaporated Al(7-Prq)$_3$ film on the device properties. DCM revealed the presence of a positive interface charge with a density of approximately 3.1 mC/m^2 in Al(7-Prq)$_3$-based OLEDs, and this positive charge governed the electron injection and accumulation properties. In addition, a high contact resistance to electron injection at the Al(7-Prq)$_3$/Ca interface was suggested, where the negative polarization charge may suppress the electron injection. The orientation polarization of the evaporated film can be controlled on the basis of the molecular structure, and it is important to determine the charge injection and accumulation properties and the potential profile of the resultant devices.

Y.N. and H.L. would like to thank members of Brütting's group (Universität Augsburg) for their kind cooperation in our experiments. We would also like to thank Nippon Steel & Sumikin Chemical Co., Ltd. for providing α-NPD and Alq$_3$ samples. This research was supported by JSPS through the "Funding Program for World-Leading Innovative R&D on Science and Technology (FIRST Program)" initiated by the Council for Science and Technology Policy, the Global-COE Project of Chiba University (Advanced School for Organic Electronics), and KAKENHI (Grant Nos. 21245042 and 22750167).

[1]D. Yokoyama, J. Mater. Chem. **21**, 19187 (2011).
[2]Y. Noguchi, Y. Miyazaki, Y. Tanaka, N. Sato, Y. Nakayama, T. D. Schmidt, W. Brütting, and H. Ishii, J. Appl. Phys. **111**, 114508 (2012).
[3]E. Ito, N. Hayashi, H. Ishii, N. Matsuie, K. Tsuboi, Y. Ouchi, Y. Harima, K. Yamashita, and K. Seki, J. Appl. Phys. **92**, 7306 (2002).
[4]N. Hayashi, K. Imai, T. Suzuki, K. Kanai, Y. Ouchi, and K. Seki, IPAP Conf. Ser. **6**, 69 (2004).
[5]N. Kajimoto, Ph.D. dissertation, Tokyo Institute of Technology, 2008.
[6]M. Kröger, S. Hamwi, J. Meyer, T. Dobbertin, T. Riedl, W. Kowalsky, and H. Johannes, Phys. Rev. B **75**, 235321 (2007).
[7]Y. Noguchi, Y. Tanaka, Y. Miyazaki, N. Sato, Y. Nakayama, and H. Ishii, "Displacement Current Measurement for Exploring Charge Carrier Dynamics in Organic Semiconductor Devices," in *Physics of Organic Semiconductors*, Second Edition, edited by W. Brütting and Ch. Adachi (Wiley-VCH, 2012), Chap. 5, pp. 119–154.
[8]Y. Okabayashi, E. Ito, T. Isoshima, and M. Hara, Appl. Phys. Express **5**, 055601 (2012).
[9]T. Isoshima, Y. Okabayashi, E. Ito, M. Hara, W. W. Chin, and J. W. Han, "Negative giant surface potential of vacuum-evaporated tris(7-propyl-8-hydroxyquinolinolato) aluminum(III) [Al(7-Prq3)] film," Org. Electron. (published online).
[10]K. Yoshizaki, T. Manaka, and M. Iwamoto, J. Appl. Phys. **97**, 023703 (2005).
[11]K. Ozasa, H. Ito, M. Maeda, and M. Hara, Appl. Phys. Lett. **98**, 013301 (2011).
[12]Y. Noguchi, N. Sato, Y. Tanaka, Y. Nakayama, and H. Ishii, Appl. Phys. Lett. **92**, 203306 (2008).
[13]W. Brütting, S. Berleb, and A. G. Mückl, Org. Electron. **2**, 1 (2001).
[14]B. Ruhstaller, S. A. Carter, S. Barth, H. Riel, W. Riess, and J. C. Scott, J. Appl. Phys. **89**, 4575 (2001).
[15]M. Matsumura, A. Ito, and Y. Miyamae, Appl. Phys. Lett. **75**, 1042 (1999).
[16]F. Rohlfing, T. Yamada, and T. Tsutsui, J. Appl. Phys. **86**, 4978 (1999).
[17]D. Taguchi, M. Weis, T. Manaka, and M. Iwamaoto, Appl. Phys. Lett. **95**, 263310 (2009).

[18]D. Taguchi, S. Inoue, L. Zhang, J. Li, M. Weis, T. Manaka, and M. Iwamoto, J. Phys. Chem. Lett. **1**, 803 (2010).
[19]G. G. Malliaras and J. C. Scott, J. Appl. Phys. **83**, 5399 (1998).
[20]T. Haskins, A. Chowdhury, R. H. Young, J. R. Lenhard, A. P. Marchetti, and L. J. Rothberg, Chem. Mater. **16**, 4675 (2004).
[21]R. H. Young, C. W. Tang, and A. P. Marchetti, Appl. Phys. Lett. **80**, 874 (2002).
[22]D. Y. Kondakov, J. R. Sandifer, C. W. Tang, and R. H. Young, J. Appl. Phys. **93**, 1108 (2003).
[23]Y. Hamada, T. Sano, M. Fujita, T. Fujii, Y. Nishio, and K. Shibata, Jpn. J. Appl. Phys., Part 2 **32**, L514 (1993).
[24]Y. Nakayama, S. Machida, Y. Miyazaki, T. Nishi, Y. Noguchi, and H. Ishii, Org. Electron. **13**, 2850 (2012).
[25]H. Ishii, K. Sugiyama, E. Ito, and K. Seki, Adv. Mater. **11**, 605 (1999).
[26]Y. Noguchi, N. Sato, Y. Miyazaki, Y. Nakayama, and H. Ishii, Jpn. J. Appl. Phys. **49**, 01AA01 (2010).
[27]Y. Tanaka, Y. Noguchi, M. Kraus, W. Brütting, and H. Ishii, Org. Electron. **12**, 1560 (2011).